American Journal of Medicine and Medical Sciences 2025, 15(12): 4501-4507
DOI: 10.5923/j.ajmms.20251512.66

Comprehensive Diagnostic Algorithm for Craniocervical Junction Anomalies: Clinical–Neurophysiological Rationale, Quantitative Indices, and Application Results

R. O. Ismailova, Sh. T. Arzikulov, A. I. Ibragimov, R. M. Yuldashev

Republican Specialized Scientific and Practical Medical Center of Neurosurgery, Tashkent, Uzbekistan

Abstract Background: Craniocervical junction (CCJ) anomalies vary widely in presentation and often combine ventral compression, posterior fossa crowding, and instability. Diagnostic pathways remain inconsistent, and isolated radiological indices do not fully capture functional impairment. Objective: To develop and evaluate a comprehensive diagnostic algorithm for CCJ anomalies integrating craniometric measurements, 3D volumetric assessment, and neurophysiological testing. Methods: Twenty-six symptomatic patients with MRI/MDCT-confirmed CCJ anomalies were studied: basilar invagination (n=6), platybasia (n=3), Chiari malformation (n=8), and Chiari with syringomyelia (n=9). Craniometric assessment included the Grabb–Oakes index, Chamberlain/McGregor/Harris lines, Redlund-Johnell & Hansson, Schmidt-Fischer angle, craniocervical angle (CVA), Klaus index, atlanto-dens interval (ADI), Cruveilhier joint, and Wackenheim line. Posterior fossa volume was analyzed using 3D CT, and dynamic MDCT was performed to detect atlantoaxial instability. Neurophysiology included BAEP interpeak latencies (RI–RV, RIII–RV) and stimulation EMG of median and tibial nerves. Results: Basilar invagination showed the greatest number of pathological craniometric indices, while platybasia primarily demonstrated reduced posterior fossa volume. Chiari malformation presented combined ventral and dorsal imbalance, and Chiari with syringomyelia exhibited the most severe neurophysiological abnormalities. BAEP prolongation and reduced peripheral conduction velocity correlated with structural severity ($p<0.05$). Conclusion: Integrating craniometry, volumetric imaging, and neurophysiology improves diagnostic accuracy and functional interpretation of CCJ anomalies. The proposed algorithm enhances risk stratification and supports individualized management, including the choice between conservative treatment, decompression, and stabilization.

Keywords Craniocervical junction, Basilar invagination, Platybasia, Chiari malformation, Syringomyelia, Craniometry, BAEP, EMG

1. Introduction

The craniocervical junction is a biomechanically loaded region where the dynamics of the skull base and upper cervical spine are combined. [1]. Small angular and distance changes can lead to significant clinical consequences (bulbar disorders, long-tract signs, instability). [2]. Despite accumulating data on the Grabb–Oakes index, Chamberlain and McGregor lines, Harris measurement, and other metrics, real-world diagnostic pathways remain heterogeneous. The lack of a unified algorithm hampers early identification of patients who should undergo decompression and/or stabilization. This work establishes a step-by-step diagnostic protocol and demonstrates its clinical–functional informativeness. Technical aspects of decompression and the role of duraplasty are widely discussed in the literature. [3], [7], [10], [9].

Received: Nov. 26, 2025; Accepted: Dec. 16, 2025; Published: Dec. 22, 2025
Published online at http://journal.sapub.org/ajmms

2. Materials and Methods

Study design: single-center case series (n=26). Inclusion criteria: confirmed CCJ anomalies on MRI/MDCT and the presence of clinical symptoms or neurophysiological deviations. Groups: basilar invagination (n=6), platybasia (n=3), Chiari malformation (n=8), and Chiari with syringomyelia (n=9). [4], [9], [17].

Neuroimaging: brain and cervical MRI (T1/T2; assessment of tonsillar ectopia, syringomyelia, medullary compression); functional MDCT of the CCJ (flexion/extension); 3D CT for posterior fossa volume calculation. Craniometry: Grabb–Oakes (normal ≤9 mm), Chamberlain (>5 mm) and McGregor (>10 mm) lines, Harris (≤12 mm), Redlund-Johnell & Hansson (≤8 mm), Schmidt-Fischer (124–127 °), CVA (145–165 °), Klaus index (30–35 mm), ADI (≤3 mm), Cruveilhier joint (≤4 mm), Wackenheim line. Neurophysiology: BAEPs (latencies RI–RV; interpeak intervals RI–RV and RIII–RV; amplitudes); stimulation EMG (conduction velocity and

M-wave amplitude) in the median and tibial nerves. Statistics: descriptive measures (mean ±SD), intergroup comparisons using two-tailed t-tests, significance set at $p<0.05$. [11], [12], [13].

3. Results

Demographic and Clinical Characteristics Mean age was 31.8 ±10.9 years; 61.5% were women. Predominant complaints: cervico-occipital pain (73%), vertigo (42%), ataxia (38%), dysarthria/dysphagia (19%). Pyramidal signs and dissociated sensory disturbances were more frequent in Chiari with syringomyelia, while static ataxia predominated in platybasia.

Craniometry and Neuroimaging The frequency of abnormalities in key metrics differed between groups. In basilar invagination, abnormal values of the Harris line, ADI, and Cruveilhier joint were more frequently observed; in Chiari malformations, combined abnormalities of the Grabb-Oakes curve, Chamberlain/McGregor lines, and dorsal balance indices (Schmidt-Fischer, CVA) were more common.

Functional MDCT in head flexion and extension enables identification of articular instabilities at the CCJ. Types of atlantoaxial dislocation on MDCT:

- Type I — Anterior atlantoaxial dislocation: the articular surfaces of the atlas (C1) are shifted anteriorly relative to the axis (C2).
- Type II — Posterior atlantoaxial dislocation: the articular surfaces of C1 are shifted posteriorly relative to C2.
- Type III — Central atlantoaxial dislocation: no obvious joint displacement on standard or dynamic images.

Table 1. Baseline characteristics by group

Parameter	All (n=26)	BI (n=6)	PB (n=3)	Chiari (n=8)	Chiari+S (n=9)
Age, years (M ±SD)	31.8 ±10.9	34.1 ±9.8	29.7 ±8.2	30.5 ±11.3	32.0 ±12.1
Women, n (%)	16 (61.5%)	4 (66.7%)	2 (66.7%)	5 (62.5%)	5 (55.6%)
Cervico-occipital pain, n (%)	19 (73%)	5 (83.3%)	2 (66.7%)	6 (75%)	6 (66.7%)
Ataxia, n (%)	10 (38%)	2 (33.3%)	2 (66.7%)	2 (25%)	4 (44.4%)
Dysphagia/dysarthria, n (%)	5 (19%)	2 (33.3%)	0	1 (12.5%)	2 (22.2%)

Note: BI — basilar invagination; PB — platybasia; Chiari — Chiari with syringomyelia. [5], [16].

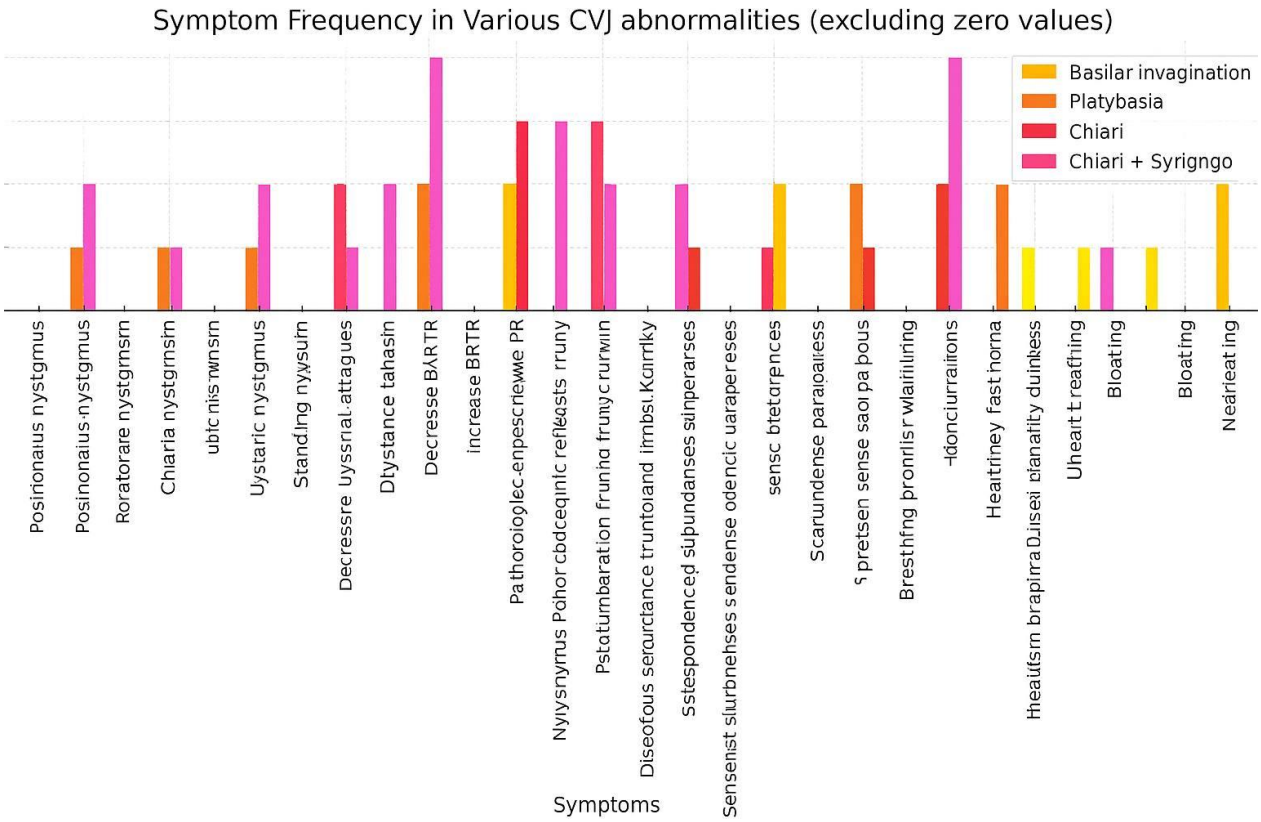

Diagram 1. Objective clinical symptoms in craniovertebral junction anomaly

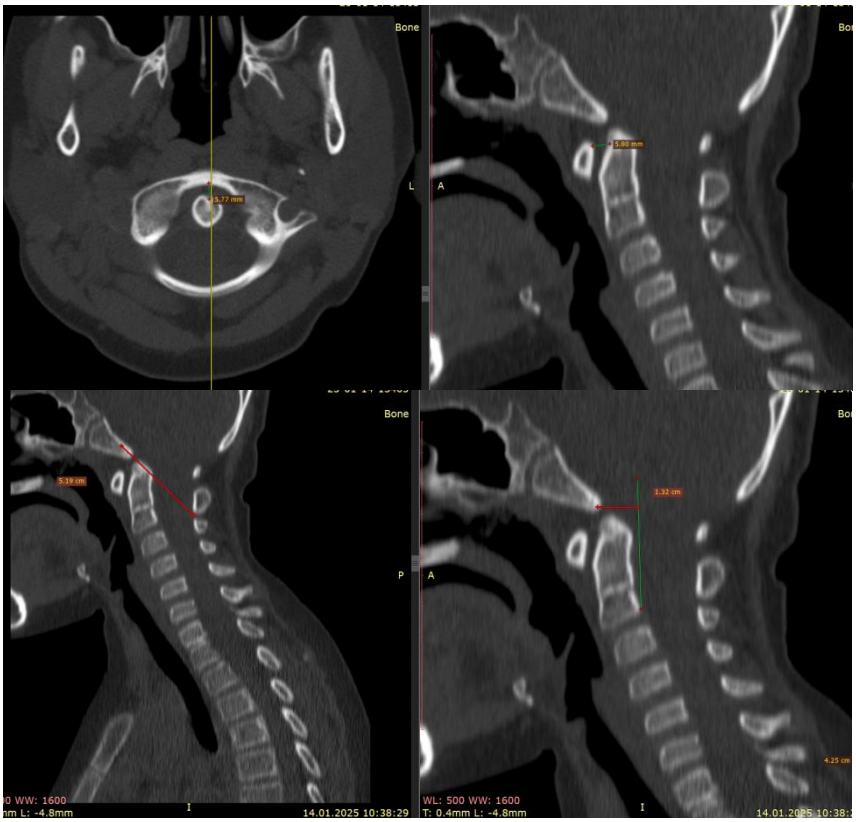

Figure 1. CT craniometric indices (Harris line, atlanto-dens interval, Wackenheim line) indicating ventral compression and craniocervical instability

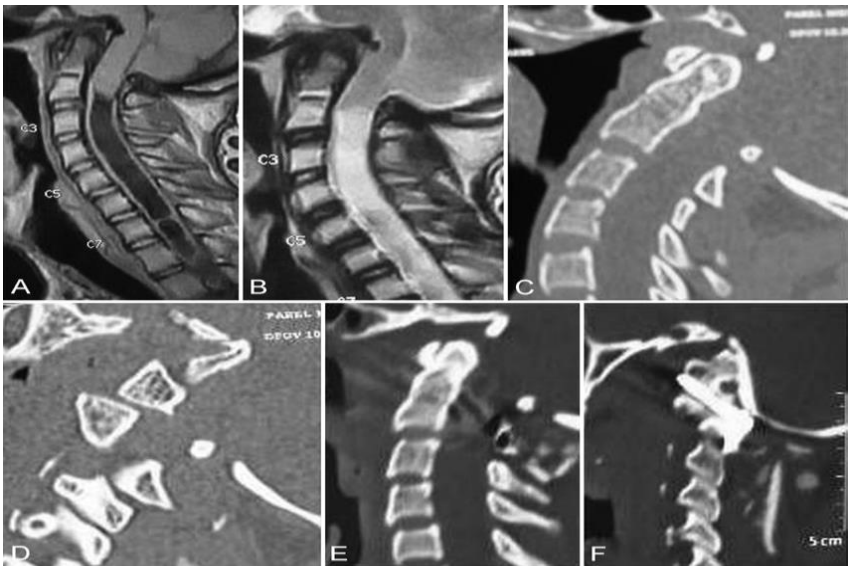

Figure 2. Types of atlantoaxial dislocation on MDCT

Table 2. Patients with pathological craniometric indices, n (%)

Index	All	BI	PB	Chiari	Chiari+S
Harris line	15 (57.7%)	6 (100%)	0	4 (50%)	5 (55.6%)
Grabb–Oakes >9 mm	14 (53.8%)	2 (33.3%)	0	5 (62.5%)	6 (66.7%)
Chamberlain/Wackenheim	14 (53.8%)	5 (83.3%)	0	5 (62.5%)	3 (33.3%)
Schmidt-Fischer	16 (61.5%)	2 (33.3%)	1 (33.3%)	6 (75%)	7 (77.8%)
CVA outside 145–165 °	15 (57.7%)	4 (66.7%)	2 (66.7%)	6 (75%)	3 (33.3%)
ADI >3 mm	9 (34.6%)	6 (100%)	0	4 (50%)	4 (44.4%)

Note: pathological thresholds are shown in parentheses; values are aligned with the study protocol.

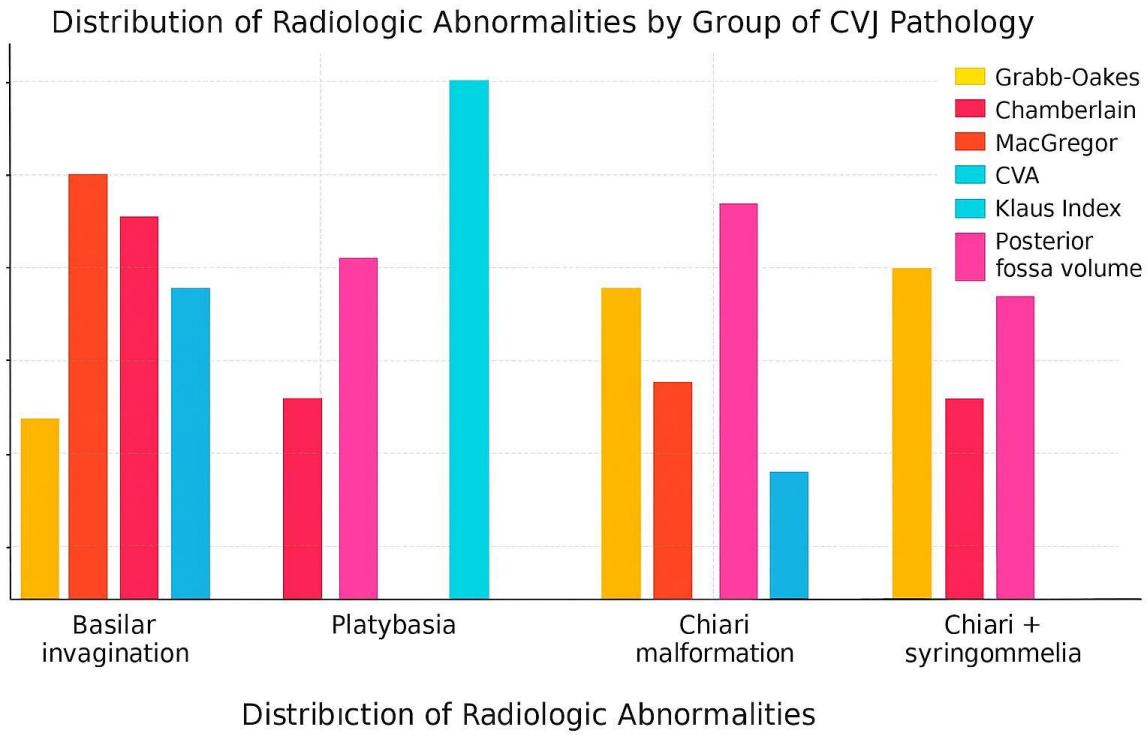

Diagram 2

Table 3. Neurophysiological parameters (M ±SD)

Parameter	Norm	BI	PB	Chiari	Chiari+S
BAEP: RI–RV, ms	4.0–4.5	4.8 ±0.3	4.5 ±0.2	4.9 ±0.4	5.1 ±0.5
BAEP: RIII–RV, ms	1.9–2.2	2.4 ±0.2	2.2 ±0.1	2.5 ±0.2	2.6 ±0.3
EMG: CV median nerve, m/s	≥50	47.2 ±3.9	49.1 ±2.8	45.8 ±4.2	43.7 ±4.5
EMG: CV tibial nerve, m/s	≥40	39.5 ±3.1	40.2 ±2.6	38.4 ±3.3	36.9 ±3.7
EMG: M-wave median nerve, mV	≥5	4.6 ±1.1	5.1 ±0.9	4.2 ±1.2	3.8 ±1.3

Note: CV — conduction velocity. Normative values are approximate for the adult population.

Diagram 2 shows how radiological abnormalities vary across key criteria in four groups of patients with CVD pathology. It illustrates this well: Maximum abnormalities across most criteria are seen in patients with basilar invagination. A significant decrease in posterior cranial fossa volume is seen only in patients with platybasia. Moderate but multiple abnormalities are seen in Chiari malformation, especially when combined with syringomyelia.

Neurophysiology (BAEP, EMG) In the Chiari and Chiari +S groups, BAEP latencies RIII and RV were prolonged, the RI–RV and RIII–RV intervals widened ($p<0.05$–0.01). EMG showed reduced conduction velocity in the median and tibial nerves, more prominent in the upper limbs; with syringomyelia, M-wave amplitudes were depressed.

Proposed Diagnostic Algorithm

1. Step 1 — Clinical screening: identify cranial nerve involvement, bulbar symptoms, pyramidal signs, ataxia, and pelvic dysfunction.
2. Step 2 — Brain and cervical MRI: determine tonsillar ectopia, syrinx length, ventral compression/odontoid retroflexion.
3. Step 3 — 3D CT/functional MDCT: calculate indices (Grabb–Oakes, Chamberlain/McGregor, Harris, Redlund-Johnell & Hansson, Schmidt-Fischer, CVA, Klaus index, ADI, Cruveilhier joint, Wackenheim line).
4. Step 4 — Neurophysiology: BAEPs and EMG for functional verification.
5. Step 5 — Stratification and management: conservative treatment if no instability; posterior fossa decompression for Chiari I without instability; decompression + stabilization when ventral compression/instability is present.

4. Discussion

Pathophysiologic context

The spectrum of craniocervical junction (CCJ) anomalies in our cohort—basilar invagination, platybasia, and Chiari I with/without syringomyelia—reflects distinct but overlapping mechanisms of brainstem compression and CSF flow

disturbance. Ventral compromise stems from odontoid retroflexion, upward migration of the dens, and occult atlantoaxial instability; dorsal crowding arises from posterior fossa underdevelopment and tonsillar ectopia. These configurations differentially load corticospinal and cerebellobulbar tracts, explaining the predominance of pyramidal signs and bulbar symptoms in ventral compression and ataxia/pain in dorsal crowding.

Structure–function correlations

We found a graded relationship between morphometry and neurophysiology. Metrics of ventral encroachment (Grabb–Oakes > 9 mm, pathological Harris, ADI > 3 mm, abnormal Wackenheim) coincided with BAEP interpeak prolongation (RI–RV, RIII–RV) and reduced motor nerve conduction velocities—changes most pronounced in the Chiari + syringomyelia subgroup. While BAEP indexes brainstem conduction, peripheral conduction slowing likely reflects segmental stress from chronic traction and microvascular compromise in the cervicomedullary junction. In platybasia, conspicuous geometric flattening did not translate into comparable BAEP change, reinforcing that location and direction of compression, not magnitude alone, determine functional impact.

Comparative perspective vs. literature

The literature underscores the limitations of single-index decision-making and the clinical heterogeneity of CCJ pathology [5–7,9]. Goel and others highlight that unrecognized atlantoaxial instability may underlie a subset of Chiari and syringomyelia, with fixation yielding clinical and radiographic improvement even without extensive decompression [16,18]. Traditional decompression-first strategies remain effective where CSF obstruction predominates without instability [7,9,10]. Our convergence of pathological Harris/ADI values with BAEP delay supports routine instability screening and argues against a one-size-fits-all approach.

Algorithm performance and triage

The proposed pathway operates as a triage funnel: (1) clinical screen, (2) MRI for tonsillar ectopia/CSF pathways, (3) 3D CT + dynamic MDCT for quantitative indices (Grabb–Oakes, Harris, Schmidt–Fischer, CVA, ADI, Wackenheim), (4) neurophysiology for functional corroboration. Concordant high-risk profiles (e.g., Grabb–Oakes > 9 mm + pathological Harris + ADI > 3 mm with BAEP delay) prioritize stabilization combined with decompression; isolated dorsal crowding with normal instability metrics favors decompression alone. Discordant results (borderline morphometry with normal BAEP) justify observation with standardized re-imaging and repeat BAEP at defined intervals.

Clinical phenotypes and thresholds

Three practical phenotypes emerged. (A) Ventral compression–instability: ADI elevation and pathological Harris with retroflexed dens and Wackenheim deviation; patients exhibit long-tract signs and greatest BAEP delay. (B) Dorsal crowding: reduced CVA and posterior fossa volume with tonsillar descent; pain and ataxia predominate, BAEP changes are mild. (C) Mixed with syringomyelia: multiple craniometric outliers and poorest neurophysiology. These map to widely used thresholds (Grabb–Oakes > 9 mm; ADI > 3 mm) and emphasize confirming borderline cases with dynamic CT before committing to fixation.

Implications for individualized management

Coupling structure with function reframes the decompression-vs-fixation choice as a testable hypothesis. In instability-dominant cases, early fixation may mitigate postoperative deterioration reported after decompression-only strategies [5]. Where dorsal crowding dominates without measurable instability, tailored decompression with duraplasty can restore CSF pulsatility and reduce syrinx volume [7,9,10]. For mixed phenotypes, sequencing fixation and decompression in a single session—or staging when anesthetic risk is high—can be guided by a composite of Grabb–Oakes, Harris/ADI, and BAEP severity. This precision approach also refines counseling about expected pain relief versus neurological recovery, which tracks with preoperative BAEP normalization potential and syrinx chronicity.

Measurement standardization and reproducibility

Given the sensitivity of angle and distance metrics to imaging planes, we advocate strict protocolization: midline sagittal MRI for Grabb–Oakes, neutral/flexion/extension MDCT for Harris/ADI/Wackenheim, and predefined threshold tables. Embedding screenshots of landmarks and storing measurement templates reduce inter-observer variance and enable longitudinal audit. Semi-automated tools for angle/line detection may further enhance reliability, particularly for Schmidt–Fischer angle and CVA.

Translational outlook

Prospective validation should link algorithmic strata to hard endpoints (gait/bulbar function, syrinx regression, re-operation rates, quality of life). The incremental value of CSF flow studies and upright MRI in borderline cases warrants study. Predictive models combining morphometrics and neurophysiology could yield individualized probability scores for instability and response to decompression versus fixation, aiding multidisciplinary decision-making and patient counseling.

Clinical Implications

- The algorithm ensures early identification of high-risk patients and reduces diagnostic delay.
- Formalized indices facilitate communication at multidisciplinary boards.
- Operation planning (decompression ± stabilization) becomes more evidence-based, potentially lowering re-operation rates.

5. Conclusions

The proposed diagnostic algorithm, based on the integration of craniometric and neurophysiological data, significantly

improves the accuracy of patient stratification with craniovertebral junction anomalies. The combined use of the Grabb-Oakes, Harris, Schmidt-Fischer, and ADI indices ensures the early detection of instability and conduction abnormalities. Furthermore, the use of standardized criteria facilitates the unification of clinical decisions and reduces the risk of over- or underdiagnosis. The obtained results confirm the importance of a multidisciplinary approach, as well as the need for further multicenter studies to clarify the prognostic value of the developed algorithm. Thus, the proposed model may become an effective tool for optimizing diagnosis, planning surgical tactics, and improving treatment outcomes for patients with craniovertebral junction anomalies.

Study Limitations

Single-center design and a limited sample reduce generalizability; no prospective validation. Long-term functional outcomes and quality of life were not assessed; multicenter protocols with unified endpoints are needed.

Ethics

The study was conducted in accordance with the Declaration of Helsinki. Local ethics approval: [RSCN 0025/27 ?03.09.2025].

Funding

Source of funding: [specify]. The sponsor had no influence on study design, data collection/analysis, manuscript preparation, or the decision to publish.

Conflict of Interest

The authors declare no conflicts of interest.

Author Contributions (CRediT)

Conceptualization and design: Sh.T. Arzikulov; Data curation: Sh.T. Arzikulov; Analysis: R.O. Ismailova; Writing: R.O. Ismailova; Sh.T. Arzikulov. Review and approval of the final version: all authors.

Data Availability

Summary data are available from the corresponding author upon reasonable request.

Abbreviations

CCJ — craniocervical junction; PF — posterior fossa; BAEP — brainstem auditory evoked potentials; EMG — electromyography; ADI — atlanto-dens interval; CVA — craniocervical angle.

REFERENCES

[1] Voronov VG. The importance of MRI and CT-AG in substantiating indications for surgical treatment of Chiari malformation in adults and children. Neurosurg Nevrol Det Vozrasta. 2010; (1): 9-21.

[2] Gushcha AO. A new minimally invasive technique for surgical treatment of Arnold-Chiari malformation: an experimental and clinical study. Russ Neurosurg J im Prof AL Polenov. 2010; (4): 23-38.

[3] Mozhaev SV, Sterlikova NV. Results of surgical treatment of Chiari malformation type I with ventrolateral localization. Ukr Neurosurg J. 2009; (3): 35.

[4] Sevostyanov DV. Chiari malformation type I: pathogenesis, diagnosis, surgical treatment (literature review). Vestn Uralsk Med Akad Nauk. 2011; (1): 63-67.

[5] Aronson DD. Instability of the cervical spine after decompression in patients who have Arnold-Chiari malformation. J Bone Joint Surg Am. 1991; 73(6): 898-906.

[6] Guo F. Surgical management of Chiari malformation: analysis of 128 cases. Pediatr Neurosurg. 2007; 43(5): 375-381.

[7] Isu T. Foramen magnum decompression with removal of the outer layer of the dura as treatment for syringomyelia occurring with Chiari I malformation. Neurosurgery. 1993; 33(5): 844-849.

[8] Levy WJ, Mason L, Hahn JF. Chiari malformation presenting in adults: a surgical experience in 127 cases. Neurosurgery. 1983; 12: 377-390.

[9] Milhorat TH, Bolognese PA. Tailored operative technique for Chiari type I malformation using intraoperative color Doppler ultrasonography. Neurosurgery. 2003; 55(4): 1008.

[10] Munshi I, Frim D, Stine-Reyes R, et al. Effects of posterior fossa decompression with and without duraplasty on Chiari malformation–associated hydromyelia. Neurosurgery. 2000; 46(6): 1384-1389.

[11] Harper CM, Daube JR. Facial nerve electromyography and other cranial nerve monitoring. J Clin Neurophysiol. 1998; 15: 206-216.

[12] Moller AR. Evoked Potentials in Intraoperative Monitoring. Baltimore, MD: Williams & Wilkins; 1988.

[13] Burke D, Hicks RG. Surgical monitoring of motor pathways. J Clin Neurophysiol. 1998; 15: 194-205.

[14] Lyon R, Feiner J, Lieberman JA. Progressive suppression of motor EP during general anesthesia: the phenomenon of anesthetic fade. J Neurosurg Anesthesiol. 2005; 17: 13-19.

[15] Dinh D, Maccall T, Matelli TA, Karanth S, Lee W. Surgical anatomy and biomechanics of the craniovertebral joint. 2016: 3-19.

[16] Goel A, Kaswa A, Shah A. Atlantoaxial fixation for treatment of Chiari formation and syringomyelia with no craniovertebral bone anomaly: experience in 57 cases. 2019: 101-110.

[17] Nishikawa M, Bolognese PA, Yamagata T, et al. Surgical management of Chiari malformation type I and instability of the craniocervical junction based on its pathogenesis and classification. 2022; 62: 400-415.

[18] Chatterjee S, Shivhare P, Verma SG. Chiari malformation and atlantoaxial instability: problems of coexistence. 2019: 1-7.

Copyright © 2025 The Author(s). Published by Scientific & Academic Publishing
This work is licensed under the Creative Commons Attribution International License (CC BY). http://creativecommons.org/licenses/by/4.0/